

The Value of 18F-PSMA-1007 PET/CT in Identifying High-Risk Prostate Cancer

Jun-jie Hong

the First Affiliated Hospital of Wenzhou Medical University

Bo-le Liu

The First Affiliated Hospital of Wenzhou Medical University

Zhi-qiang Wang

the First Affiliated Hospital of Wenzhou Medical University

Kun Tang

the First Affiliated Hospital of Wenzhou Medical University

Xiao-wei Ji

the First Affiliated Hospital of Wenzhou Medical University

Wei-wei Yin

the First Affiliated Hospital of Wenzhou Medical University

Jie Lin

the First Affiliated Hospital of Wenzhou Medical University

Xiang-wu Zheng (✉ zxwu111@sina.com)

The First Affiliated Hospital of Wenzhou Medical University

Original research

Keywords: 18F-PSMA-1007, Prostate cancer, High risk

Posted Date: June 19th, 2020

DOI: <https://doi.org/10.21203/rs.3.rs-34968/v1>

License:  This work is licensed under a Creative Commons Attribution 4.0 International License.

[Read Full License](#)

Abstract

Background: Clinical management decisions on prostate cancer (PCa) are often based on a determination of risk. ^{68}Ga -prostate-specific membrane antigen (PSMA)-11-positron-emission-tomography (PET)/ computer-tomography (CT) is an attractive modality to assess biochemical recurrence of PCa, detect metastatic disease and stage of primary PCa, making it a promising strategy for risk stratification. However, due to some limitation of ^{68}Ga -PSMA-11 the development of alternative tracers is of high interest. In this study, we aimed to investigate the value of the new PET trace ^{18}F -PSMA-1007 in identifying high-risk PCa.

Methods: 170 patients with primary PCa underwent ^{18}F -PSMA-1007 PET/CT were retrospectively analyzed. According to the European Association of Urology (EAU) guidelines on prostate cancer for PCa, patients were classified into low-intermediate-risk (LMR) group or high-risk (HR) group. The maximum standardized uptake values (SUV_{max}) of the primary prostate tumor was measured on PET/CT images. The diagnostic performance of PET/CT for LMR and HR PCa were calculated and the relationship between the SUV_{max} of primary prostate tumor, prostate-specific antigen (PSA) level and Gleason score (GS) were analyzed.

Results: Of all 170 patients, 55 patients were classified into LMR group and 115 patients were classified into HR group. There was a significant positive correlation between the PSA level/GS and SUV_{max} ($r = 0.597$, $r = 0.446$, $P < 0.001$, respectively). Tumors with GS of 6 and 7a showed significantly lower ^{18}F -PSMA-1007 uptake compared to patients with GS of 8, 9, and 10 ($P < 0.001$). SUV_{max} in patients of HR was significantly higher than those of LMR (median SUV_{max} : 20.20 versus 8.40; $P < 0.001$). In receiver operating characteristic (ROC) curve analysis, the optimal cutoff value of the SUV_{max} for identifying high-risk PCa was set as 10.78 (area under the curve [AUC]: 0.873; sensitivity: 90.4%; specificity: 69.1%).

Conclusion: ^{18}F -PSMA-1007 PET/CT showed the powerful diagnosis efficacy for high-risk PCa, which can be used as an objective imaging reference index for clinical reference.

Background

PCa is one of the most common tumors in men worldwide [1]. Patients with those high-risk features (defined by the EAU guidelines on prostate cancer as T2c disease and/or sum Gleason score > 7 and/or serum PSA > 20 ng/ ml) predict a higher risk of metastasis, recurrence or death. The conventional method of identifying high-risk disease in the preliminary diagnosis fails to meet clinical needs. There is a need to develop new methods to allow for appropriate risk stratification for management, such as active surveillance programs, definitive therapy, prostatectomy, radiotherapy, or up-front androgen-deprivation. Incorporation of imaging to current primary PCa classifications for risk stratification can help achieve that unmet clinical need [2].

PSMA is a membrane-bound enzyme with high expression in prostate cancer cells and low expression in benign prostatic tissue [3]. Over the past few years, targeted imaging of PSMA has been used in various clinical managements, such as imaging-guided biopsy, staging of primary tumor, localization of biochemical relapse, planning of radiotherapy, prediction, and assessment of tumor response to systemic therapy [4–7]. The PSMA expression level of PCa and tumor level, Gleason score and PSA stage before treatment had been proved definitely correlated, and the expression levels have been found to be a predictor for PCa progression [8–10]. PSMA-based PET/CT has also been reported to be enabling better tumor detection rate than standard radiologic imaging procedures [11].

Currently, ^{68}Ga -PSMA-11 is a widely used tracer for PET imaging applications in the detection of PCa. Nevertheless, the disadvantage of ^{68}Ga -PSMA PET/CT is that it has more bladder activity, as tracer accumulation in the urinary tract may influence the uptake evaluation of the prostate bed [12]. Recently, the new PSMA tracer, ^{18}F -PSMA-1007, can eliminate this kind of disadvantage because of its hepatobiliary excretion owing to its moderate lipophilic characteristics. It has been used as a promising new PET tracer in the management of PCa [13, 14]. Furthermore, ^{18}F -PSMA-1007 has longer half-life and higher physical spatial resolution than ^{68}Ga -PSMA PET/CT, because ^{18}F is cyclotron-produced with the larger activity amount [13]. In previous studies, ^{18}F -PSMA-1007 had been reported that the intensity of tracer accumulation in the primary tumors of PCa patients correlated to GS and PSA level, and it is promising for accurate local staging of PCa [13, 15, 16]. Furthermore, it has similar or better diagnostic performance than ^{68}Ga -PSMA-11 in local recurrence or metastasis [14, 17]. However, the major limitation of the studies was the relatively small number of patients, and there is limited published data on the diagnosis efficacy of ^{18}F -PSMA-1007 PET/CT for high-risk PCa.

Thus, we intended to measure the intensity of tracer uptake in the primary prostate tumor and evaluate the value of ^{18}F -PSMA-1007 PET/CT noninvasive imaging diagnostic strategies to identify the high-risk of PCa and tried to establish an objective imaging reference index.

Materials And Methods

Patients

In this retrospective study, we analyzed the medical records of 170 PCa patients with Gleason Score of 6 or greater who underwent ^{18}F -PSMA-1007 PET/CT imaging at our institution between March 2019 and May 2020. The study group included 116 patients with 12-core random, transrectal ultrasound-guided (TRUS) biopsy-proven prostate cancer and 54 patients with radical prostatectomy (RP). In all patients, the time interval between the measurements of PSA values to ^{18}F -PSMA-1007 PET/CT scan was less than four weeks. Patients were excluded if they received local or systemic treatment, and had the previous history of other cancer. According to the EAU guidelines on prostate cancer [18], all patients were divided into low-intermediate-risk (LMR) group or high-risk (HR) group. The patients of the LMR need to meet all of the following criteria: (1) $\text{PSA} \leq 20 \text{ ng/ml}$; (2) Gleason score 6 - 7; (3) cT1 - cT2b. As the same, the

patients of the HR need to meet at least one of the following criteria: (1) PSA > 20 ng/ml; (2) Gleason score 8 - 10; (3) above cT2c. Due to the retrospective nature of the study, no formal approval from the ethics committee was required according to our national legislation.

Radiopharmaceutical

^{18}F -PSMA-1007 precursor, cassettes and reagents for the synthesis of ^{18}F -PSMA-1007 were obtained from ABX advanced biochemical compounds (Radeberg, Germany). ^{18}F -PSMA-1007 was prepared in a GE TracerLab FN synthesizer according to the one-step procedure described previously [19]. The radiochemical purity of the final product was >90% as determined by high-performance liquid chromatography.

Imaging Protocol

^{18}F -PSMA-1007 images were acquired from a body PET/CT scanner (Gemini 64 TF, Philips Medical Systems, Best, The Netherlands) and were performed approximately 120 minutes after IV injection of 4.0 MBq/kg ^{18}F -PSMA-1007 (median activity: 282.7 MBq; range: 170.2–366.3 MBq). For attenuation correction, a low-dose unenhanced CT scan was performed from the skull base to the middle of the thigh, with the following parameters: tube voltage of 140 Kvp, tube current of 110 mA, detector collimation of 64×0.625 mm, pitch of 0.829, a tube rotation speed of 0.5 s, section thickness of 5 mm and reconstruction thickness of 2.5 mm, and was followed by the PET scan that matched the CT section thickness. A three-dimensional mode was used to obtain PET images with the following parameters: field of view, 576 mm; matrix of 144×144 ; slice thickness and interval, 5 mm. The emission scan time for each bed position was 1.5 min and the overlap between two adjacent bed positions was 50%.

Image analysis

All ^{18}F -PSMA PET/CT images were analyzed using a dedicated workstation (EBW3.0, Philips), which allowed the review of PET, CT and fused imaging data in axial, coronal and sagittal slices. PET imaging was interpreted independently by 2 experienced nuclear medicine physicians both of whom have more than 10 years of clinical experience and blind of all relevant clinical statistics. Any disagreement was resolved by consensus.

SUV_{max} of the primary tumors were acquired from the most intense uptake area in prostate gland. Areas in the whole body having uptake above the background activity were defined as metastatic. Typical pitfalls such as PSMA uptake in sacral and coeliac ganglia or in the stellate ganglia were frequently observed but were not considered pathological [20]. This interpretation criterion comes from the result of our clinical experience and consistent with published literature [21-24].

Statistical analysis

Data analyses were performed with SPSS version 23.0 software (SPSS, Chicago, IL). Associations between GS, PSA value, and SUV_{max} of the primary tumor were described descriptively (Nonparametric Spearman correlation coefficients). The differences between different subgroups were evaluated by using the Mann–Whitney U test and Kruskal–Wallis test. ROC curve analysis was used to determine the optimal cutoff value of the SUV_{max} for identifying high-risk PCa. For all statistical parameters, P values of less than 0.05 were considered statistically significant.

Results

Patients' Characteristics

The clinical characteristics of the enrolled 170 patients with GS 6 to 10 are summarized in Table 1. Among the 170 patients, the median age was 71 years (43–89 years). The proportions of patients enrolled in different subgroups were 67.6% and 32.4% for HR vs. LMR. All patients presented with a median PSA value of 20.041 ng/ml before the PET/CT scan (range: 0.970–2980.629 ng/ml). The median SUV_{max} of all tumors was 16.05 (range: 4.80–81.10). (showed in Table 1)

Table 1
Patient characteristics

Patients(n)	170
Age median (range)	71 years (43–89)
PSA median (range)	21.240 ng/ml (0.970-2980.629)
LMR(n)	55
HR(n)	115
GS	
GS 6	12
GS 7a	22
GS 7b	45
GS 8	25
GS 9	50
GS 10	16
N, number; LMR, low-Intermediate-risk group; HR, high-risk group	
GS, Gleason score; GS 7a corresponds to GS 3 + 4; GS 7b corresponds to GS 4 + 3	

Correlation analysis

There was a statistically significant difference in median SUV_{max} between patients of HR and those of LMR (20.20 vs. 8.40, $P < 0.001$; Table 2). For the Gleason score, the detailed information about the SUV_{max} values of different GS subgroups are summarized in Table 3. Gleason score and SUV_{max} of primary tumors showed a significant positive correlation with each other ($r = 0.446$, $P < 0.001$). Combining GS and tumor-related tracer uptake, lower median SUV_{max} value was found in the subgroups GS 6 (SUV_{max} : 5.86) and GS 7a (SUV_{max} : 8.76) than in GS 7b (SUV_{max} : 14.30), GS 8 (SUV_{max} : 18.60), GS 9 (SUV_{max} : 20.49) and GS 10 (SUV_{max} : 24.45). The result of Kruskal–Wallis test showed that the differences in SUV_{max} value between tumors with GS of 6 and 7a and those with GS of 8, 9 and 10 were statistically significant ($P < 0.001$, respectively). Figure 1 and 2 showed two examples for a GS 6 and a GS 9 PCa. A comparison of SUV_{max} for all GS subgroups was illustrated in Figure 3. In terms of PSA level, there was a significant and strong positive correlation between the PSA value and the corresponding SUV_{max} value of the primary tumors ($r = 0.597$, $P < 0.001$).

Table 2
SUVmax value and PSA level of the primary tumor in different risk groups

	N	SUV_{max}, Median(range)	SUV_{max}, Mean \pm SD	PSA, Median(range)	PSA, Mean \pm SD
LMR	55	8.40(4.80–30.80)	10.21 \pm 5.50	8.149(0.970–32.280)	8.956 \pm 4.047
HR	115	20.20(6.40–81.10)	25.26 \pm 15.79	34.623(2.326–2980.629)	131.651 \pm 343.414

Table 3
SUVmax value of all primary prostate cancer in different Gleason score subgroups

	N	SUV_{max}, Median(range)	SUV_{max}, Mean \pm SD
GS 6	12	5.86(4.80–18.30)	7.83 \pm 3.69
GS 7a	22	8.76(4.80–21.60)	9.79 \pm 4.48
GS 7b	45	14.30(5.12–77.70)	16.52 \pm 11.67
GS 8	25	18.60(7.40–81.10)	30.02 \pm 21.46
GS 9	50	20.49(6.40–69.20)	25.59 \pm 14.48
GS 10	16	24.45(8.70–43.70)	23.99 \pm 8.36
Total	170	16.05(4.80–81.10)	20.39 \pm 15.10

ROC Curve Analysis

Figure 4 showed the result of the ROC curve analysis for high-risk PCa. The AUC of the SUV_{max} was 0.873. The sensitivity and specificity were 90.4% and 69.1%, respectively. The optimal cut-off values of SUV_{max} was set as 10.78.

Discussion

In this retrospective study, we found that there is a certain positive correlation between the intensity of ^{18}F -PSMA-1007 accumulation and the GS/PSA level in the primary tumors of PCa patients. Furthermore, the SUV_{max} of the primary tumor was valuable for identifying high-risk PCa.

A timely and accurate diagnosis of high-risk PC is front and center for the clinician. The commonly used risk classification for the PC are based on clinical stage, Gleason score by biopsy, and PSA level before treatment. However, it is not absolutely reliable to evaluate the accuracy of GS in patients who have undergone TURP. In the clinical work, it may also encounter the patient who refuse biopsy for a variety of reasons. Another problem with the scheme is the inherent inaccuracy in determining T stage [2]. Assessing disease by digital rectal examination has significant inter-observer variability. PSMA-PET/CT, as a noninvasive imaging diagnostic strategy, may compensate for these shortcomings. Recent studies found a statistically significant positive correlation between GS/PSA value and SUV_{max} of primary tumors on PSMA-PET/CT [13, 23]. Kesch et al. proved ^{18}F -PSMA-1007 PET/CT and multiparametric magnetic resonance imaging had similar diagnostic performance in local staging of PCa [15]. In our study, the SUV_{max} showed a significant association with the presence of high-risk PCa. Patients of HR had significantly higher SUV_{max} than those of LMR ($P < 0.001$). The AUC of the SUV_{max} of the primary tumor is 0.873, which can efficaciously identify high-risk patients with PCa. Therefore, we believe pathologists and clinicians may reduce missed diagnoses if they refer to PET images and results. Besides, PSMA-PET/CT may better screen out the patients of high risk, especially when the patients are unable to receive aspiration biopsy or the histology results of biopsy are not satisfactory.

The biological characteristics of PCa tissues vary greatly between different GS, which is an important indicator for the treatment and prognosis evaluation of PCa [18]. Thus, we also made the pairwise comparison between different GS subgroups and found that there were statistically significant differences in SUV_{max} between the subgroups of GS 6 and GS 7a, and the subgroups of GS 8–10 ($P < 0.001$). There was no statistical difference in SUV_{max} value between tumors with 7b and those with GS of 8–10, which was different from the result of previous studies on ^{68}Ga -PSMA [23, 24]. Reasons for these discrepancies remain speculative. The pathological results of TRUS-biopsy may underestimate the actual Gleason scores, which might be one of the reasons. Previous study had shown that compared with the subgroup GS 7b, the dangerous level of the subgroup GS 7a tumors could be treated conservatively without the need for a radical surgery [25], thus, the distinguishment between the two subgroups is of great importance for clinical treatment. But it is worth noting that the SUV_{max} of primary tumor between these two subgroups has no statistical difference with a median SUV_{max} of 8.76 (GS 7a) and 14.30 (GS 7b), ($P > 0.05$). This finding was consistent with previous studies on ^{68}Ga -PSMA [23, 24], which may

reveal that the stage difference between GS 7a and GS 7b was not enough to cause a difference in SUV_{max} on PSMA-PET/CT.

The present study had some limitations that should not be neglected. Firstly, the retrospective nature of the analysis is the major limitation of our study, and further validation is required by multicenter studies with more patients. Secondly, the patients of histopathological confirmation account for a larger proportion of all patients, thus, there might be a possibility that the histology results of primary tumors were underestimated in some of the enrolled patients. Finally, histopathological confirmation was not acquired for metastatic lesions in this study.

Conclusion

In conclusion, ^{18}F -PSMA-1007 was a great potential tracer for PCa PET/CT imaging. The intensity of tumor-related tracer uptake on ^{18}F -PSMA-1007 PET/CT correlates with the PSA level and GS in primary PCa. Furthermore, ^{18}F -PSMA-1007 PET/CT showed powerful diagnostic performance for risk stratification of primary PCa, which can be used as a reference index for identifying high-risk PCa.

Abbreviations

PCa: Prostate Cancer

EAU: European Association of Urology

PSA: Prostate Specific Antigen

GS: Gleason score

PSMA: Prostate Specific Membrane Antigen

LMR: Low-intermediate-risk

HR: High-risk

SUV_{max} : The maximum standardized uptake values

PET-CT: Positron Emission Tomography/Computed Tomography

TRUS: Transrectal ultrasound

RP: Radical Prostatectomy

ROC: Receiver operating characteristic

AUC: Area under the curve

Declarations

Ethics approval and consent to participate

All procedures performed in studies involving human participants were in accordance with the ethical standards of the institutional and/or national research committee and with the 1964 Helsinki Declaration and its later amendments or comparable ethical standards. Due to the retrospective nature of the study, no formal approval from the ethics committee was required according to our national legislation.

Consent for publication

Not applicable

Availability of data and material

The datasets used and/or analyzed during the current study are available from the corresponding author on reasonable request.

Competing interests

All authors declare that they have no competing interests.

Funding

No funding was obtained for the present study.

Authors' contributions

Jun-jie Hong: data acquisition, literature research, and manuscript writing. Bo-le Liu, Xiao-wei Ji, Wei-wei Yin and Jie Lin: data acquisition and review, Kun Tang: study design and theoretical support. Xiang-wu Zheng and Zhi-qiang Wang: design of the research program, review and revise of manuscript. All the authors agreed on the content of the final manuscript.

Acknowledgements

Not applicable.

Authors' information (optional)

Jun-jie Hong and Bo-le Liu contributed equally to this work.

Affiliations:

Department of PET/CT, The First Affiliated Hospital of Wenzhou Medical University, Xuefu North Rd, Wenzhou, Zhejiang, 325000, People's Republic of China.

Jun-jie Hong & Bo-le Liu & Zhi-qiang Wang & Kun Tang & Xiao-wei Ji & Wei-wei Yin & Jie Lin & Xiang-wu Zheng

Correspondence to: Xiang-wu Zheng, MD, Department of PET/CT, Radiology Imaging Center, The First Affiliated Hospital of Wenzhou Medical University, Xuefu North Rd, Wenzhou, Zhejiang, 325000, People's Republic of China.

E-mail: zxwu111@sina.com

References

1. Siegel RL, Miller KD, Jemal A. Cancer statistics. 2019. *CA Cancer J Clin.* 2019;69:7–34. doi:10.3322/caac.21551.
2. Chang AJ, Autio KA, Roach M 3rd, Scher HI. High-risk prostate cancer-classification and therapy. *Nat Rev Clin Oncol.* 2014;11:308–23. doi:10.1038/nrclinonc.2014.68.
3. Kasperzyk JL, Finn SP, Flavin R, Fiorentino M, Lis R, Hendrickson WK, et al. Prostate-specific membrane antigen protein expression in tumor tissue and risk of lethal prostate cancer. *Cancer Epidemiol Biomarkers Prev.* 2013.
4. Afshar-Oromieh A, Avtzi E, Giesel FL, Holland-Letz T, Linhart HG, Eder M, et al. The diagnostic value of PET/CT imaging with the (68)Ga-labelled PSMA ligand HBED-CC in the diagnosis of recurrent prostate cancer. *Eur J Nucl Med Mol Imaging.* 2015;42:197–209. doi:10.1007/s00259-014-2949-6.
5. Rahbar K, Weckesser M, Huss S, Semjonow A, Breyholz HJ, Schrader AJ, et al. Correlation of Intraprostatic Tumor Extent with 68 Ga-PSMA Distribution in Patients with Prostate Cancer. *J Nucl Med.* 2016;57:563–7. doi:10.2967/jnumed.115.169243.
6. Giesel FL, Will L, Lawal I, Lengana T, Kratochwil C, Vorster M, et al. Intraindividual Comparison of (18)F-PSMA-1007 and (18)F-DCFPyL PET/CT in the Prospective Evaluation of Patients with Newly Diagnosed Prostate Carcinoma: A Pilot Study. *J Nucl Med.* 2018;59:1076–80. doi:10.2967/jnumed.117.204669.
7. Rahman LA, Rutagengwa D, Lin P, Lin M, Yap J, Lai K, et al. High negative predictive value of 68 Ga PSMA PET-CT for local lymph node metastases in high risk primary prostate cancer with histopathological correlation. *Cancer Imaging.* 2019;19:86. doi:10.1186/s40644-019-0273-x.
8. Bravaccini S, Puccetti M, Bocchini M, Ravaioli S, Celli M, Scarpi E, et al. PSMA expression: a potential ally for the pathologist in prostate cancer diagnosis. *Sci Rep.* 2018;8:4254. doi:10.1038/s41598-018-22594-1.
9. Fendler WP, Eiber M, Beheshti M, Bomanji J, Ceci F, Cho S, et al. (68)Ga-PSMA PET/CT: Joint EANM and SNMMI procedure guideline for prostate cancer imaging: version 1.0. *Eur J Nucl Med Mol Imaging.* 2017;44:1014–24. doi:10.1007/s00259-017-3670-z.
10. Ross JS, Sheehan CE, Fisher HA, Kaufman RP Jr, Kaur P, Gray K, et al. Correlation of primary tumor prostate-specific membrane antigen expression with disease recurrence in prostate cancer. *Clin*

- Cancer Res. 2003;9:6357–62.
11. Maurer T, Gschwend JE, Rauscher I, Souvatzoglou M, Haller B, Weirich G, et al. Diagnostic Efficacy of (68)Gallium-PSMA Positron Emission Tomography Compared to Conventional Imaging for Lymph Node Staging of 130 Consecutive Patients with Intermediate to High Risk Prostate Cancer. *J Urol*. 2016;195:1436–43. doi:10.1016/j.juro.2015.12.025.
 12. Afshar-Oromieh A, Malcher A, Eder M, Eisenhut M, Linhart HG, Hadaschik BA, et al. PET imaging with a [68Ga]gallium-labelled PSMA ligand for the diagnosis of prostate cancer: biodistribution in humans and first evaluation of tumour lesions. *Eur J Nucl Med Mol Imaging*. 2013;40:486–95. doi:10.1007/s00259-012-2298-2.
 13. Giesel FL, Hadaschik B, Cardinale J, Radtke J, Vinsensia M, Lehnert W, et al. F-18 labelled PSMA-1007: biodistribution, radiation dosimetry and histopathological validation of tumor lesions in prostate cancer patients. *Eur J Nucl Med Mol Imaging*. 2017;44:678–88. doi:10.1007/s00259-016-3573-4.
 14. Rahbar K, Weckesser M, Ahmadzadehfar H, Schafers M, Stegger L, Bogemann M. Advantage of (18)F-PSMA-1007 over (68)Ga-PSMA-11 PET imaging for differentiation of local recurrence vs. urinary tracer excretion. *Eur J Nucl Med Mol Imaging*. 2018;45:1076–7. doi:10.1007/s00259-018-3952-0.
 15. Kesch C, Vinsensia M, Radtke JP, Schlemmer HP, Heller M, Ellert E, et al. Intraindividual Comparison of (18)F-PSMA-1007 PET/CT, Multiparametric MRI, and Radical Prostatectomy Specimens in Patients with Primary Prostate Cancer: A Retrospective, Proof-of-Concept Study. *J Nucl Med*. 2017;58:1805–10. doi:10.2967/jnumed.116.189233.
 16. Giesel FL, Knorr K, Spohn F, Will L, Maurer T, Flechsig P, et al. Detection Efficacy of (18)F-PSMA-1007 PET/CT in 251 Patients with Biochemical Recurrence of Prostate Cancer After Radical Prostatectomy. *J Nucl Med*. 2019;60:362–8. doi:10.2967/jnumed.118.212233.
 17. Giesel FL, Kesch C, Yun M, Cardinale J, Haberkorn U, Kopka K, et al. 18F-PSMA-1007 PET/CT Detects Micrometastases in a Patient With Biochemically Recurrent Prostate Cancer. *Clin Genitourin Cancer*. 2017;15:e497-e9. doi:10.1016/j.clgc.2016.12.029.
 18. Cornford P, Bergh RCN, Briers E, Santis M, Fanti S, Gillessen S, et al. EAU-EANM-ESTRO-ESUR-SIOG Guidelines on Prostate Cancer 2020 published guidelines. 2020.
 19. Cardinale J, Martin R, Remde Y, Schafer M, Hienzsch A, Hubner S, et al. Procedures for the GMP-Compliant Production and Quality Control of [(18)F]PSMA-1007: A Next Generation Radiofluorinated Tracer for the Detection of Prostate Cancer. *Pharmaceuticals (Basel)*. 2017;10. doi:10.3390/ph10040077.
 20. Backhaus P, Noto B, Avramovic N, Grubert LS, Huss S, Bogemann M, et al. Targeting PSMA by radioligands in non-prostate disease-current status and future perspectives. *Eur J Nucl Med Mol Imaging*. 2018;45:860–77. doi:10.1007/s00259-017-3922-y.
 21. Ceci F, Uprimny C, Nilica B, Geraldo L, Kendler D, Kroiss A, et al. (68)Ga-PSMA PET/CT for restaging recurrent prostate cancer: which factors are associated with PET/CT detection rate? *Eur J Nucl Med*

- Mol Imaging. 2015;42:1284–94. doi:10.1007/s00259-015-3078-6.
22. Sachpekidis C, Kopka K, Eder M, Hadaschik BA, Freitag MT, Pan L, et al. 68 Ga-PSMA-11 Dynamic PET/CT Imaging in Primary Prostate Cancer. *Clin Nucl Med*. 2016;41:e473-e9. doi:10.1097/RLU.0000000000001349.
23. Ergul N, Yilmaz Gunes B, Yucetas U, Toktas MG, Cermik TF. 68 Ga-PSMA-11 PET/CT in Newly Diagnosed Prostate Adenocarcinoma. *Clin Nucl Med*. 2018;43:e422-e7. doi:10.1097/RLU.0000000000002289.
24. Uprimny C, Kroiss AS, Decristoforo C, Fritz J, von Guggenberg E, Kendler D, et al. (68)Ga-PSMA-11 PET/CT in primary staging of prostate cancer: PSA and Gleason score predict the intensity of tracer accumulation in the primary tumour. *Eur J Nucl Med Mol Imaging*. 2017;44:941–9. doi:10.1007/s00259-017-3631-6.
25. Epstein JI, Zelefsky MJ, Sjoberg DD, Nelson JB, Egevad L, Magi-Galluzzi C, et al. A Contemporary Prostate Cancer Grading System: A Validated Alternative to the Gleason Score. *Eur Urol*. 2016;69:428–35. doi:10.1016/j.eururo.2015.06.046.

Figures

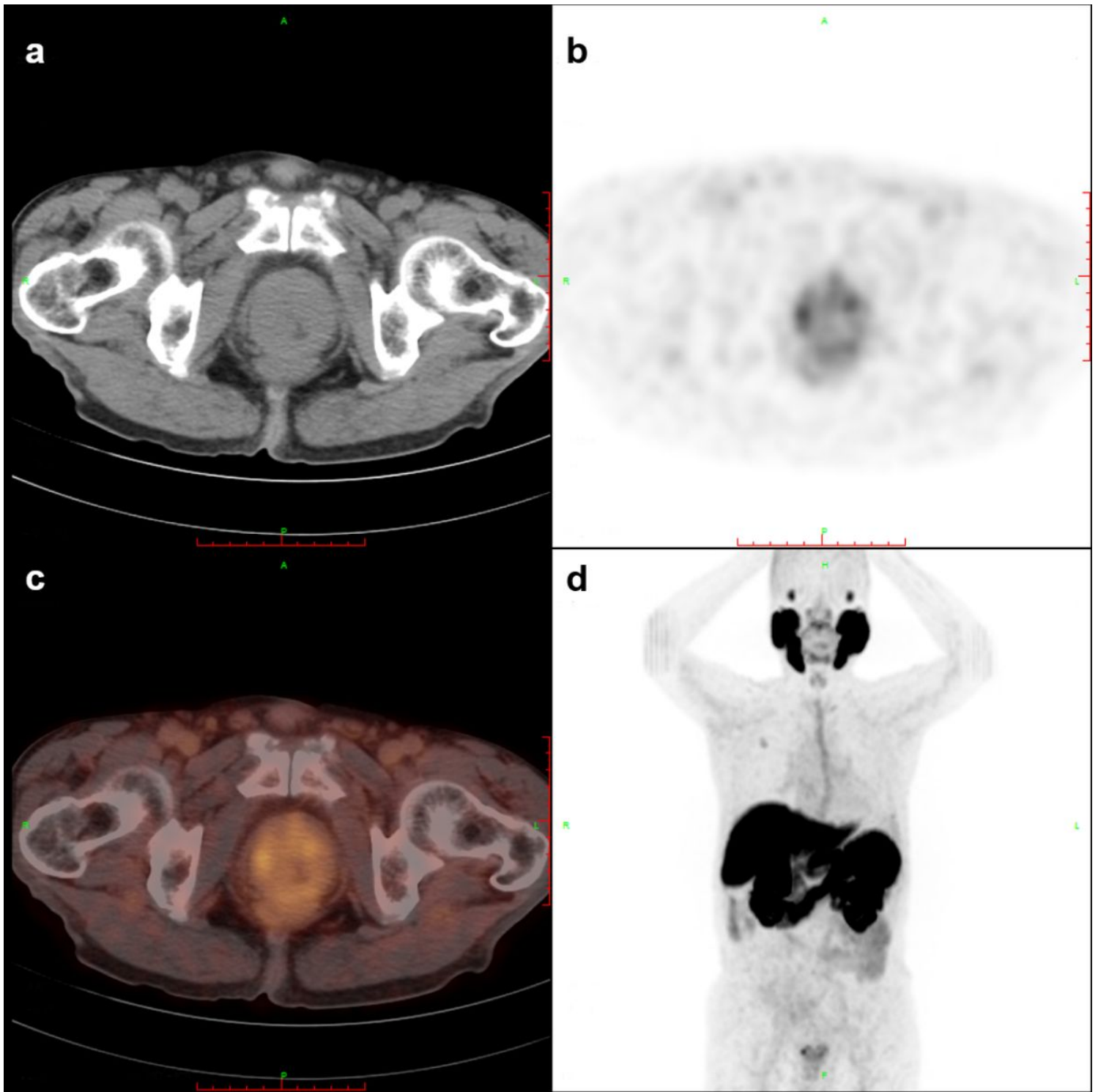


Figure 1

18F-PSMA-1007 PET/CT with CT (a), axial PET (b), fused PET/CT (c) and maximum-intensity projection (d) images of an 80-year-old patient with biopsy proven PCa (GS 6) and a PSA value of 12.011ng/ml. This patient was classified into LMR group. Axial PET (b) and fused PET/CT (c) images showed light scattered 18F-PSMA-1007 uptake in both sides of prostate gland (SUVmax of 6.50).

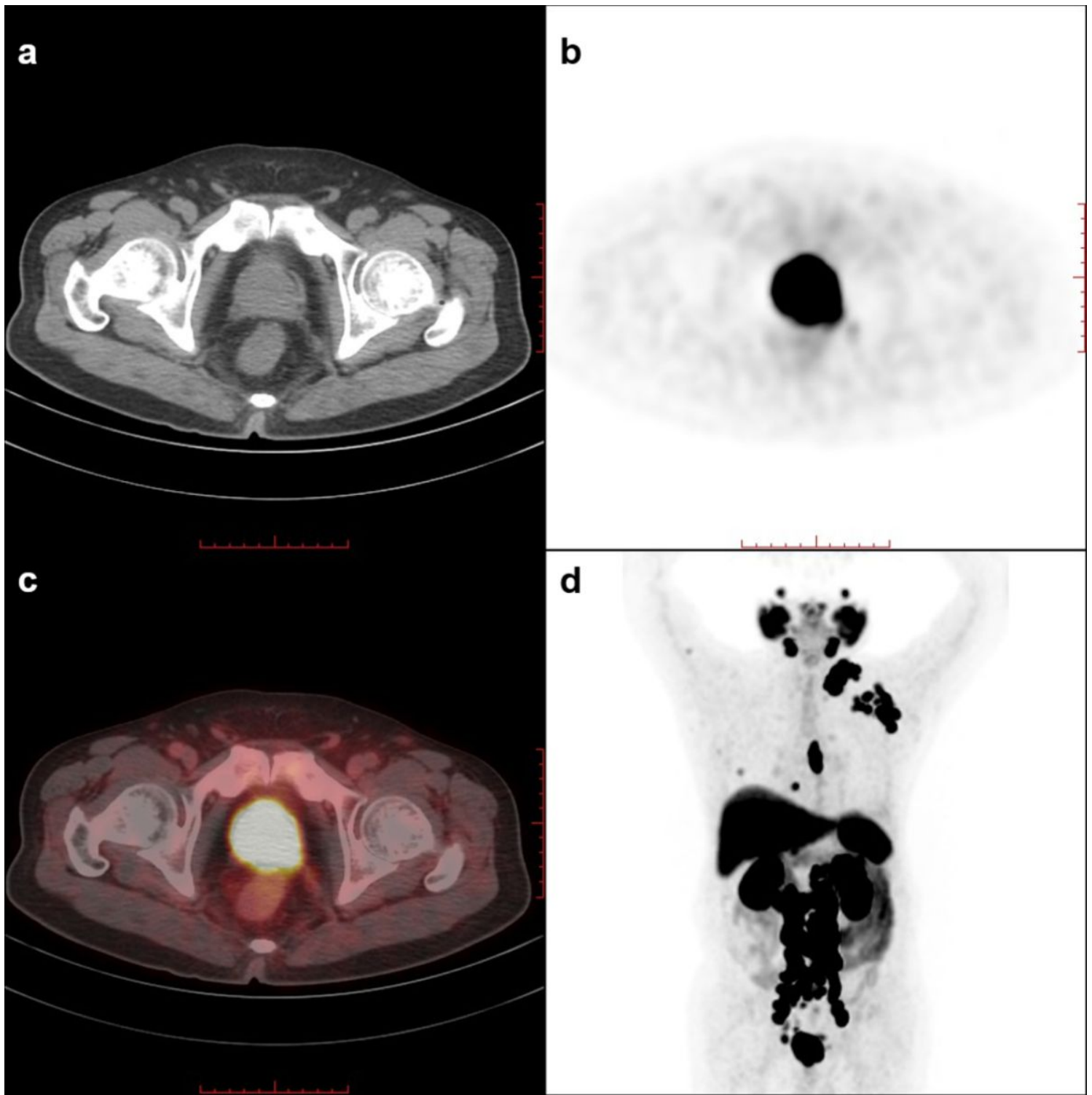


Figure 2

18F-PSMA-1007 PET/CT with CT (a), axial PET (b), fused PET/CT (c) and maximum-intensity projection (d) images of a 79-year-old patient with biopsy proven PCa (GS 9) and a PSA value of 1220.000ng/ml. This patient was classified into HR group. Axial PET (b), fused PET/CT (c) images showed diffuse hypermetabolism in the prostate gland (SUVmax: 69.20). Maximum-intensity projection (d) image showed multiple lymphatic metastases (SUVmax: 85.00) and bone metastases (SUVmax: 12.70).

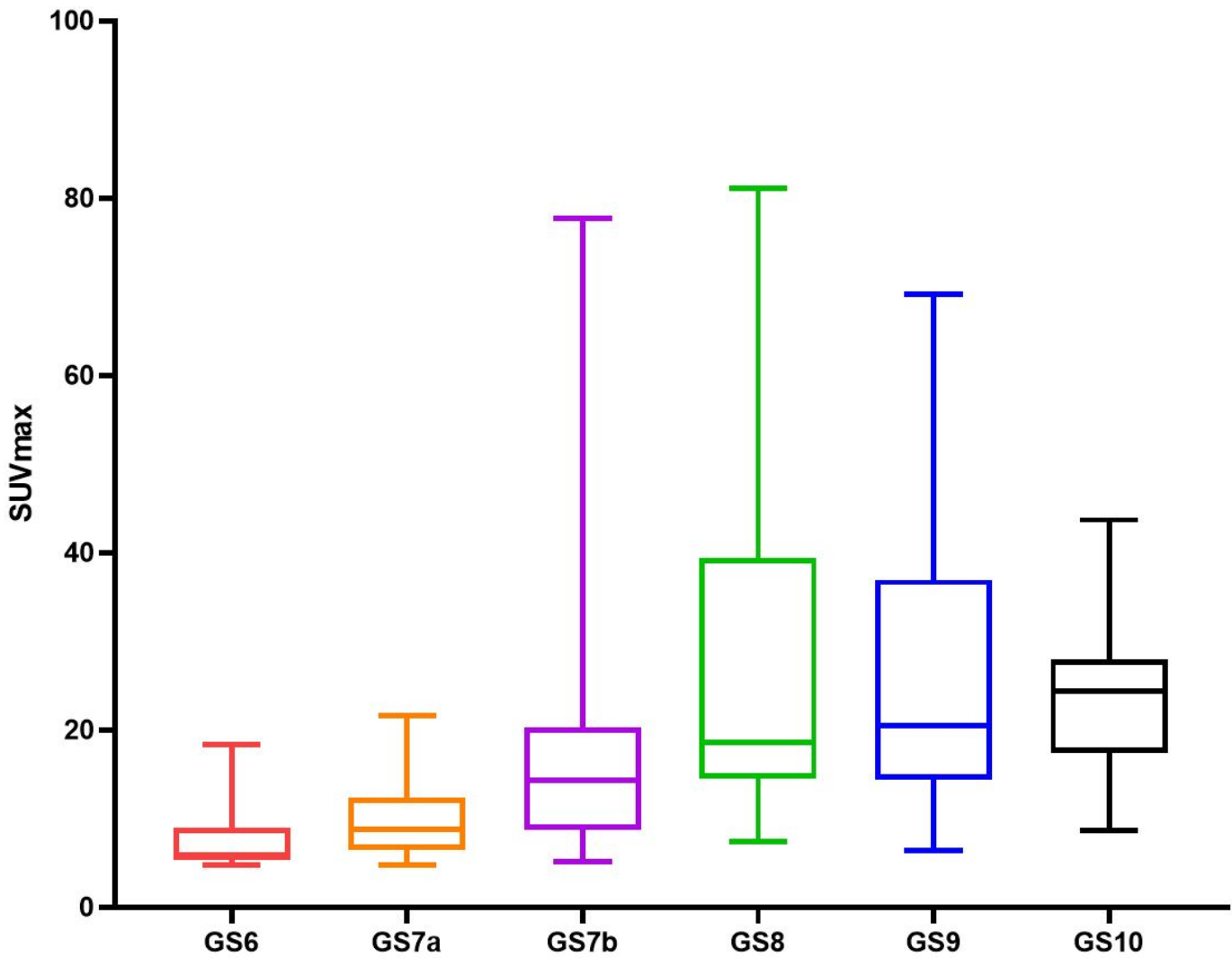


Figure 3

Comparison of ¹⁸F-PSMA-1007 uptake expressed in SUVmax value in primary tumors of different GS subgroups. Box plots demonstrate that higher GS exhibited statistically significant higher tracer uptake in the primary tumor.

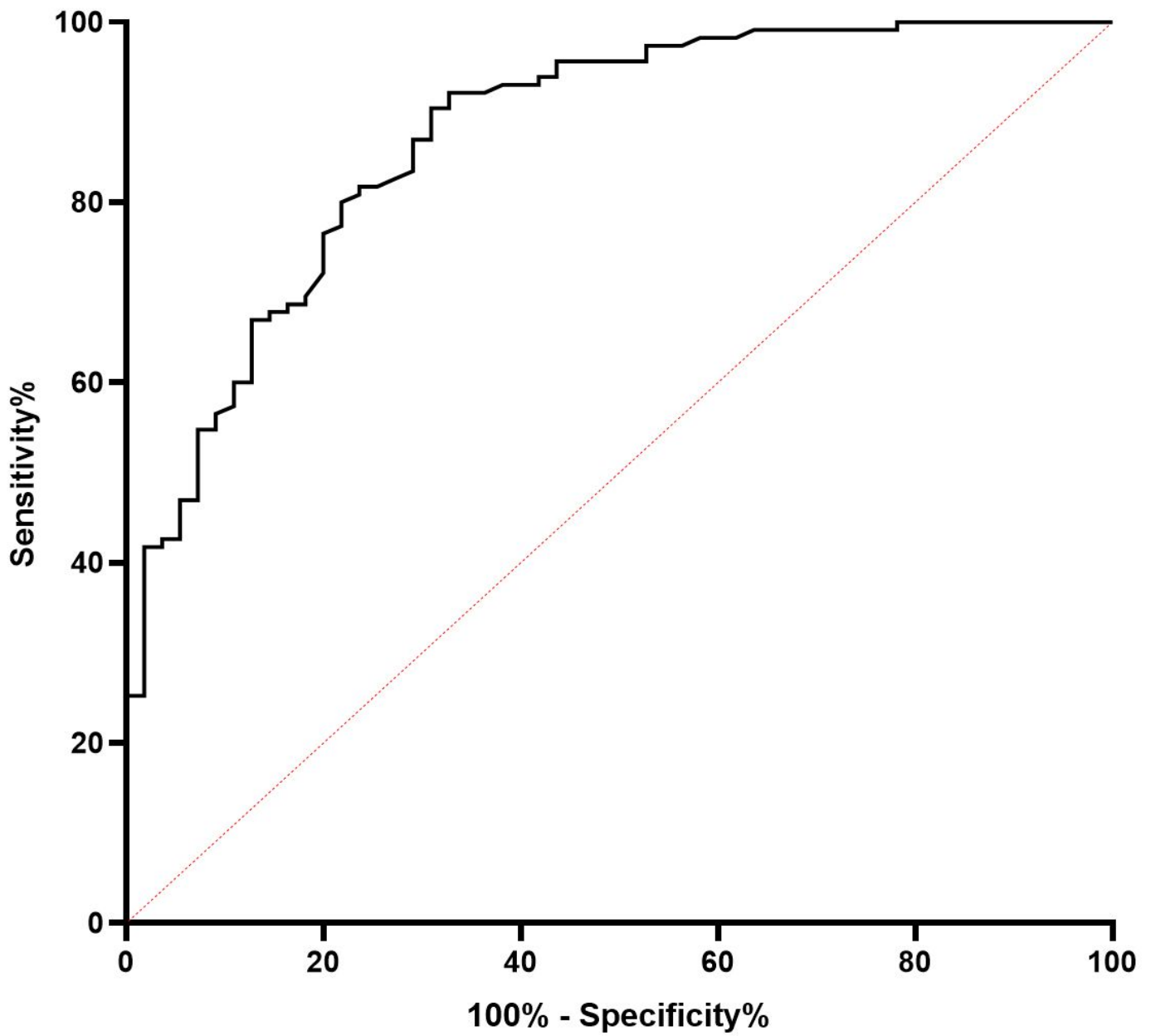


Figure 4

ROC curve of the SUVmax for high-risk prostate cancers. 95% confidence interval [CI], 0.8167 – 0.9289; P < 0.001, sensitivity: 90.4%; specificity: 69.1%